

DETECTION OF X-RAY FLUORESCENCE LINE FEATURE FROM THE LUNAR SURFACE

Y. Kamata¹, T. Takeshima², T. Okada³, and K. Terada⁴

¹ *Research Center for Advanced Energy Conversion, Nagoya University, Furo-cho, Chikusa-ku,
Nagoya 464-8602 Japan*

² *NASA Goddard Space Flight Center (Universities Space Research Association), Greenbelt, MD 20771, USA*

³ *The Institute of Space and Astronautical Science, Sagami-hara, Kanagawa 229-8510 Japan*

⁴ *Department of Earth and Planetary Systems Science, Faculty of Science, Hiroshima University,
Kagami-yama 1-3-1, Higashi-Hiroshima, Hiroshima 739 Japan*

ABSTRACT

We present the results of an analysis by ASCA (Japanese X-ray astronomy satellite) observation of the lunar surface on July 10th - 11th, 1993. In spite of the fact that the X-ray surface brightness is estimated to be at nearly CXB (Cosmic X-ray Background) level, the X-ray spectrum shows significant deviations in relation to Al-K α and Si-K α fluorescence X-rays. According to the intensity ratios of Al/Si (1-2) and Mg/Si (<0.4), the properties of the X-ray spectrum is consistent with an intermediate abundance ratio between highlands and mares (or relatively similar to highland values). However, the X-ray illuminated region on the lunar surface are mainly covered with mare regions and the emission of Al-K and Si-K fluorescence arises from both day side and night side region of the moon. These facts indicate the existence of X-ray production due to bremsstrahlung, with high energy particles impacting even on the night side.

INTRODUCTION

When X-ray astronomy started more than 30 years ago, an X-ray observation of scattered solar X-rays was performed by a sounding rocket almost to no avail because of the low sensitivity of the instruments. During the Apollo missions (15-16), the observation of the fluorescent X-rays of Mg-K, Al-K and Si-K covering 10% of the lunar surface was done by filtered proportional counters (Clark *et al.* 1976, Adler and Trombka 1977, Clark and Trombka 1997, Clark and Adler 1978). These observations reveal that there is a significant positive correlation between visual albedos and Al/Si X-ray intensity ratios which is also confirmed by the sample analysis of lunar rocks (Clark *et al.* 1976, 1978, Hubbard and Keith 1977). This means that highland regions are Al rich relative to mare regions.

In the beginning of the 1990s, the PSPC instrument on board ROSAT satellite showed the shadowing of Cosmic X-ray Background (CXB) by the moon, in the 0.1-2 keV energy band. The soft X-ray image of the moon shows an excess emission component even from the night side, as high as 25 times the internal background level and 2 orders of magnitude weaker than the bright side component (Schmitt *et al.* 1991). These results infer that there exist low energy (in the range of a few hundred eV) electron impacts which produce the observed soft X-rays even on the dark side (Schmitt *et al.* 1991). In order to investigate the origin of these X-rays, we analyzed the data in the 0.7-10 keV energy band obtained with the Japanese X-ray Astronomy Satellite, ASCA on July 10-11, 1993.

ASCA OBSERVATION AND DATA ANALYSIS

The observation was carried out using two different X-ray detectors, the SIS (Solid state Imaging Spectrometer) and the GIS (Gas Imaging Spectrometer), with energy resolutions of ~2% and ~8% at 6keV, respectively and four sets of the high throughput X-ray mirror assemblies with a total effective area of more than 1000 cm² at 1.5 keV (Burke *et al.* 1991, Tanaka *et al.* 1994, Serlemitsos *et al.* 1995, Ohashi *et al.* 1996) in the 0.5-10keV energy band. The observation was done by pointing mode as the moon passed through the field of view with a typical speed of 2 arcmin/minute. The total exposure of the 11 pointing observations was 50 ks, while the effective exposure of the moon was about 5 ks. The X-ray spectra of the GIS and SIS instruments for this analysis are integrated for an offset angle between the lunar geometric center and the center of FOV (field of view) of less than 15 arcmin.

On the other hand, X-ray images were made from various offset images in respect to the lunar positions in the FOV.

We summed up aspect corrected X-ray images for each 1 minute using both GIS and SIS, resulting in a typical spatial resolution of 2-3 arcmin due to the effect of movement and blurring of X-ray mirrors.

RESULTS

X-Ray Spectra..

We applied spectral fitting using 5 model components, namely the CXB (power-law with fixed index of 1.56), solar scattered X-rays ($\log T=6.2$; Clark and Adler 1978), Mg-K (1.25 keV), Al-K (1.49 keV) and Si-K (1.74 keV). The integrated X-ray spectra of GIS and SIS and the results of the spectral fits are shown in figure 1a-b and table 1

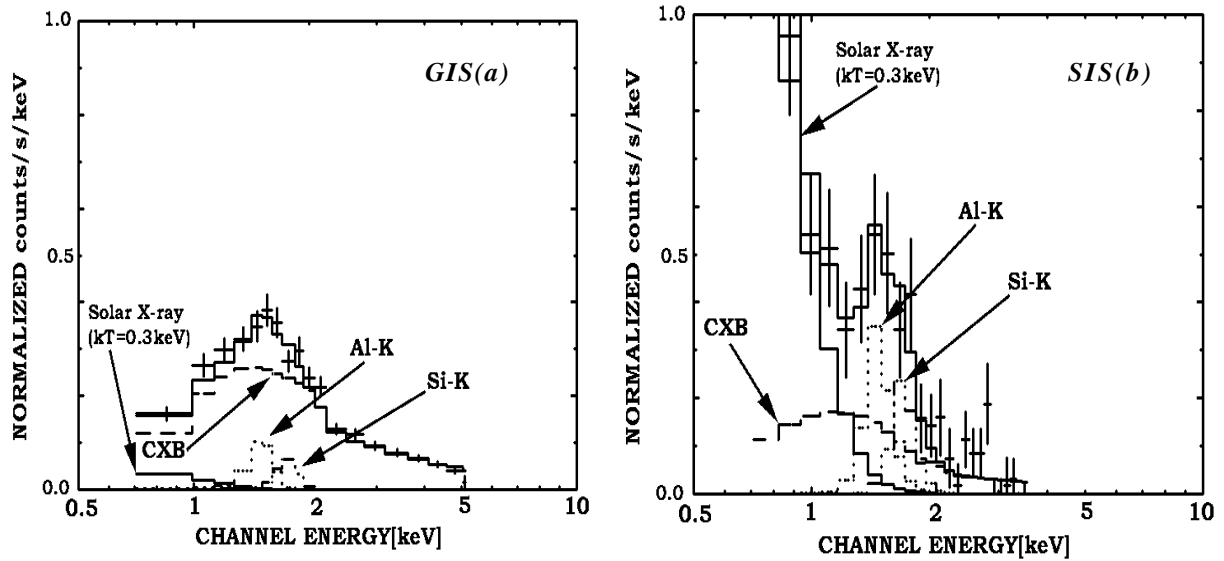


Fig. 1. The integrated X-ray spectra of GIS(a) and SIS(b) instruments. The graphs show normalized X-ray flux [$c/s/keV$] VS photon energy [keV]. Crosses and lines denote observed data points and model spectra of solar back scattered components, Cosmic X-ray Background, and fluorescent lines as shown in the figure.

Noting that the effective geometric area ($22 \times 22'$) of the SIS detector is nearly 30% smaller than that of GIS detector (30 arcmin in diameter), the obtained intensities of fluorescent lines are found to be consistent with each other. The normalizations of the CXB and solar scattered components were difficult to estimate because of the complicated X-ray mirror response function (Tsusaka *et al.* 1995) against the diffuse emission, due to the fact that CXB was obscured by the moving moon in the field of view in addition to the solar component illuminating half of the moon.

On the other hand, the intensity ratios between fluorescent lines are almost independent of these effects. By estimating the absolute contribution of these line intensities and dividing by a factor of 2 due to the movement of the moon, a total line contribution (Al-K and Si-K) of $\sim 1 \times 10^{-5}$ [photons/s/cm²] is obtained.

Table 1. Line Intensities (Errors are 90% confidence level)

Element	I(SIS) [$\times 10^{-5}$ photons/s/cm ²]	I(GIS) [$\times 10^{-5}$ photons/s/cm ²]
Mg	<5.0	<10
Al	9 \pm 5	13 \pm 5
Si	7.5 \pm 5.0/ \pm 4.5	6 \pm 4
reduced ²	0.968(dof=20)	1.41(dof=89)

X-Ray Surface Brightness Distribution.

Following the data reduction discussed above, X-ray surface brightness distribution images of GIS in the 0.7-2 keV and of SIS in the 1.3-1.6 keV energy band were done. The former (GIS; less energy resolution of ~8%) image shows the distribution of Al-K and Si-K fluorescence together with scattered solar X-rays, and the latter (SIS; higher energy resolution of ~2%) shows the distribution of Al-K fluorescence which is equivalent to the distribution of typical rocks and soils in highland regions (Clark *et al.* 1976). The images are shown in figure 2a-b.

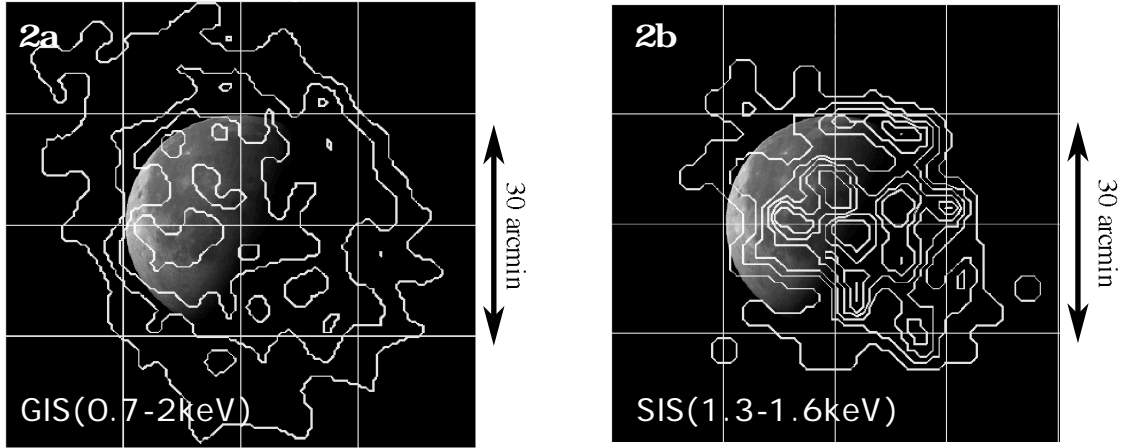


Fig. 2. The contours of X-ray surface brightness distribution of GIS(a) and SIS(b) instruments in the 0.7-2 keV and in the 1.3-1.6 keV energy band overlaid on the visual image of the moon, after the aspect correction to the lunar center, respectively. These images are smoothed with Gaussian function of $\sigma = 2.5$ arcmin which corresponds to twice a typical spatial resolution. Grid intervals in both images are equivalent to 15 arcmin and contour levels are linearly scaled.

Figure 2a shows the half moon structure in the X-ray band indicating the solar scattered component in the day side of the moon; figure 2b shows a relatively uniform surface brightness distribution both on the bright and the dark side of the moon, implying that the Al-K fluorescence lines are uniformly generated independently of the X-ray illumination by solar radiation.

DISCUSSION

Chemical Composition of the Elements.

Intensity ratios of Mg/Si and Al/Si are good indicators of the types of lunar rocks and soils (Adler and Trombka 1977). The next step considered of estimating intensity ratios and element abundances from the results of spectral fits as shown in table 2. Although these results involve major uncertainties, Al/Si(element) ratio of 0.5-0.9 is intermediate of value between the typical highland value of 0.8-0.9 and the mare value of 0.25, with an upper limit of a Mg/Si ratio that is relatively small (Adler and Trombka 1977).

Table 2. Intensity Ratios and Element Abundance Ratios

ratio	SIS(confidence level)	GIS(confidence level)
Al/Si(intensity)	1.2 \pm 0.6(68%)	2.2 \pm 1.1(68%)
Al/Si(element)	0.5 \pm 0.3(68%)	0.9 \pm 0.5(68%)
Mg/Si(intensity)	<0.4(90%)	<1.0(90%)
Mg/Si(element)	<0.1(90%)	<0.3(90%)

Origin of Fluorescence Lines.

The characteristics of intensity ratios of fluorescence lines are similar to those of intermediate ones between

highlands and mares; on the other hand, the illuminated area on the lunar surface is mainly covered with mare (2/3) during the observation period (lunar phase ~ 0.6). In addition, the SIS image of the Al-K fluorescence line shows a roughly uniform surface brightness distribution, which is a tracer of the highland component. These facts indicate the existence of bremsstrahlung production of fluorescence X-rays by impacts of charged particles, higher in energy than the Al-K edge of 1.56 keV. The total observed fluorescence (Al-K and Si-K) by a photon flux of $\sim 1 \times 10^{-4}$ [photons/s/cm²] is equivalent to an X-ray production of more than 10^{18} [photons/s]. Low-Z optically thick materials produce $\sim 10^{-4}$ photons per one electron or $\sim 10^{-5-8}$ photons per one high energy proton (>200 keV) impact with higher energy than K-edge energy (Dyson 1990).

Assuming incident electrons of >2 keV in energy (beyond K-edge energy), the estimated electron or proton impacts amount to $>10^{22}$ [electrons/s] or $>10^{23-26}$ [protons/s] onto the lunar surface. Hence, in this case, the particle flux against lunar surface is estimated to be $>10^4$ [electrons/s/cm²] or $>10^{5-8}$ [protons/s/cm²]. The previous observations by Apollo 15-16 indicate the electron flux to be $\sim 10^{3-4}$ [electrons/s/sr/cm²] (Anderson 1972a, 1972b) due to the interpolation of the measurements in the 1.9-2.1keV and 5.9-6.4keV energy bands, which is consistent with our estimated electron flux. On the other hand, the observed proton flux at 2-3AU at polar region of the sun is estimated to be $\sim 10^{-2}$ [protons/s/cm²/sr/MeV] in the 0.48-1.2MeV (Lanzerotti et al. 1996) or $\sim 10^{-1}$ [protons/s/cm²/sr/MeV] at 1AU from the sun. This value is extremely low value assuming uniform proton flux from the sun. Then the interpretation of electron bombardments is in good agreement with our observational results.

The accurate estimation depends on the species of charged particles, their energy distribution function, time variabilities, the lunar surface geometry, and also the solar X-ray illumination on the bright side of the moon. In addition, possibilities such as galactic cosmic ray interactions or internal radio activities of the surface material are also candidates of origin of X-rays. These results are expected to be achieved in the future on an on-going mission such as the Lunar Prospector (NASA/USA) and/or SELENE (ISAS&NASDA/Japan).

ACKNOWLEDGMENTS

The data analysis was fully supported by the X-ray astronomy group, Department of Astrophysics, Nagoya University. The authors are thankful to the group members, as well as to the members of the software development team of NASA/GSFC and ISAS (Japan), and to the people who took great efforts in the daily operation of the ASCA satellite among the Japanese X-ray astronomy groups.

REFERENCES

- Adler, I., and Trombka, J.I. Phys. Chem. Earth. Vol. **10**, 17 (1977)
- Anderson, K.A., L.M. Chase, R.P. Lin, J.E. McCoy, and R.E. McGuire, "Subsatellite Measurements of Plasmas and Solar Particles". Chapter 21, in Apollo 15 Preliminary Science Report, NASA/SP-289 (1972a)
- Anderson, K.A., L.M. Chase, R.P. Lin, J.E. McCoy, and R.E. McGuire, "Subsatellite Measurements of Plasma and Energetic Particles". Chapter 22, in Apollo 16 Preliminary Science Report, NASA/SP-315 (1972b)
- Burke, B.E., Mountain, R.W., Harrison, D.C., Bautz, M.W., Doty, J.P., Ricker, G.R., and Daniels, P.J., IEEE Trans ED-**38**, 1069 (1991)
- Clark, P.E., Andre, C.G., Adler, I., Podwysoccki, M., and Weidner, J. Geophys. Res. Let. Vol. **3**, No.8, 421 (1976)
- Clark, P.E., and Adler, I. Proc. Lunar Planet. Sci. Conf. 9th, 3029 (1978)
- Clark, P.E., Eliason, E., Andre, C.G., and Adler, I. Proc. Lunar Planet. Sci. Conf. 9th, 3015 (1978)
- Clark, P.E., and Trombka, J.I. J. Geophys. Res., Vol. **102**, No.E7, 16361 (1997)
- Dyson, N.A. 'X-rays in atomic and nuclear physics', Cambridge University Press (1990)
- Hubbard, N.J., and Keith, J.E. Proc. Lunar Planet. Sci. Conf. 8th, 909 (1977)
- Lanzerotti, L.J., MacLennan, C.G., Armstrong, T.P., Roelof, E.C., Gold, R.E., and Decker, R.B. A&A, 316, 457-463 (1996)
- Ohashi, T., Ebisawa, K., Fukazawa, Y., Hiyoshi, K., Horii, M. *et al.* PASJ **48**, 157 (1996)
- Schmitt, J.H.M.M., Snowden, S.L., Aschenbach, B.A., Hasinger, G., Pfeiffermann, E. *et al.* Nature Vol. **349**, 583 (1991)
- Serlemitsos, P.J., Jalota, L., Soong, Y., Kunieda, H., Tawara, Y. *et al.* PASJ **47**, 105 (1995)
- Tanaka, Y., Inoue, H., and Holt, S.S. PASJ **46**, L37 (1994)
- Tsusaka, Y., Suzuki, H., Yamashita, K., Kunieda, H., Tawara, Y. *et al.* Appl. Opt. **34**, 4848 (1995)